Supporting information

Coordination-driven self-assembly of ruthenium(II) architectures: Synthesis, characterization and cytotoxicity studies

Aderonke Ajibola Adeyemo[a], Abhijith Shettar[b,c], Imtiyaz Ahmad Bhat[a], Paturu Kondaiah[b*], Partha Sarathi Mukherjee[a]*

[a]Department of Inorganic and Physical Chemistry, Indian Institute of Science, Bangalore 560012, India; Tel.: +91-80-22933352; Fax: +91-80-23601552; E-mail: psm@iisc.ac.in.

[b]Department of Molecular Reproduction, Development and Genetics, Indian Institute of Science, Bangalore 560012, India; Tel.: +91-80-22932688; Fax: +91-80-23600999; E-mail: paturu@iisc.ac.in.

[c]Department of Biotechnology Engineering, Ramaiah Institute of Technology, Bangalore-560064

*__Corresponding authors__: psm@iisc.ac.in; paturu@iisc.ac.in.

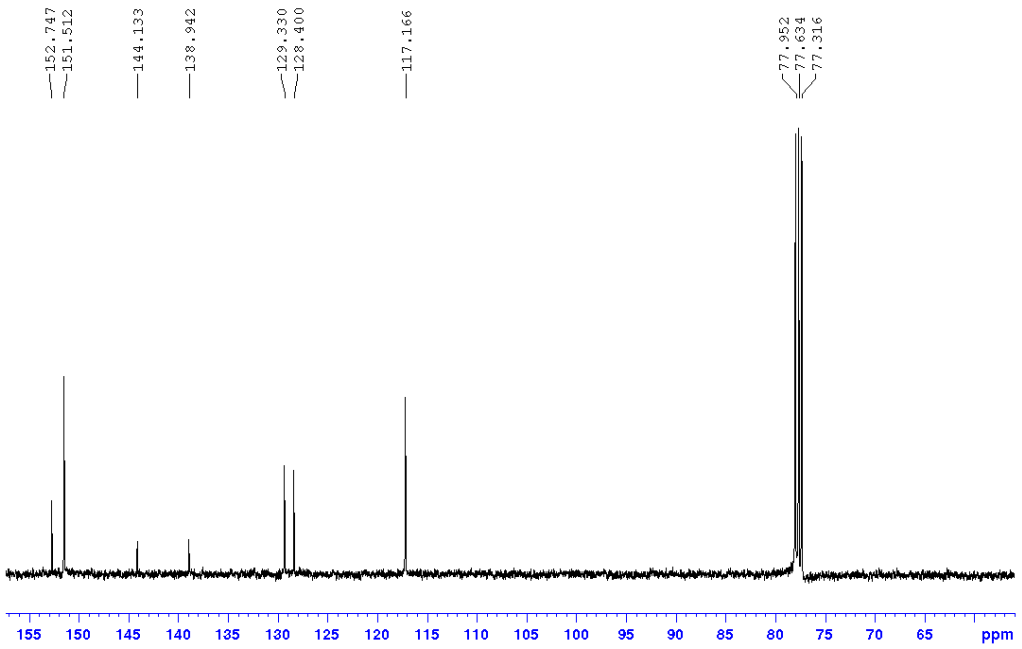

Fig. S1. ^{13}C NMR spectrum of **TD** in $CDCl_3$ at room temperature.

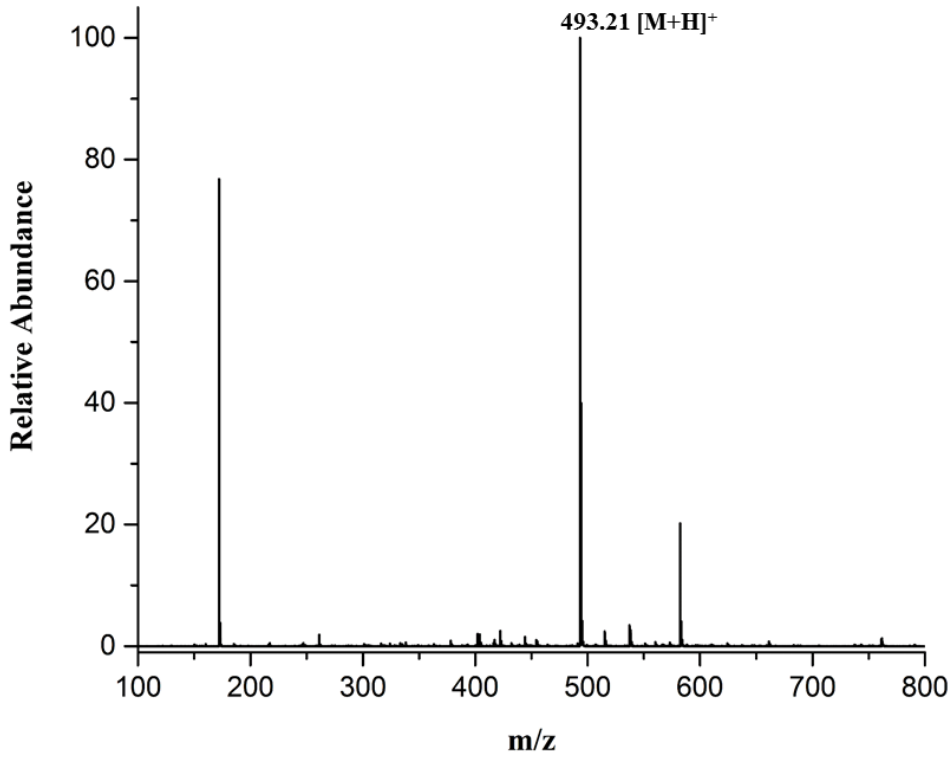

Fig. S2. ESI-MS spectrum of **TD** in methanol.

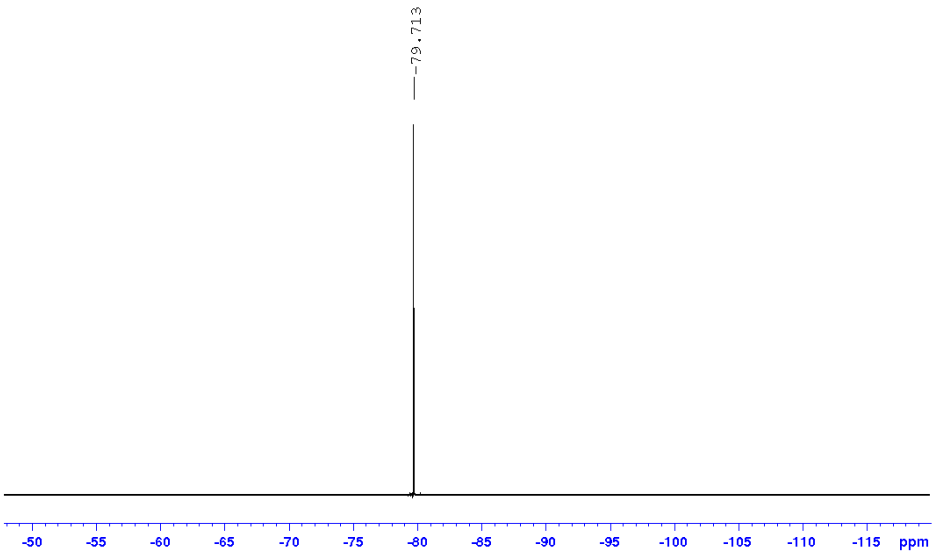

Fig.S3. ^{19}F NMR spectrum of **MA$_1$** in CD_3OD at room temperature.

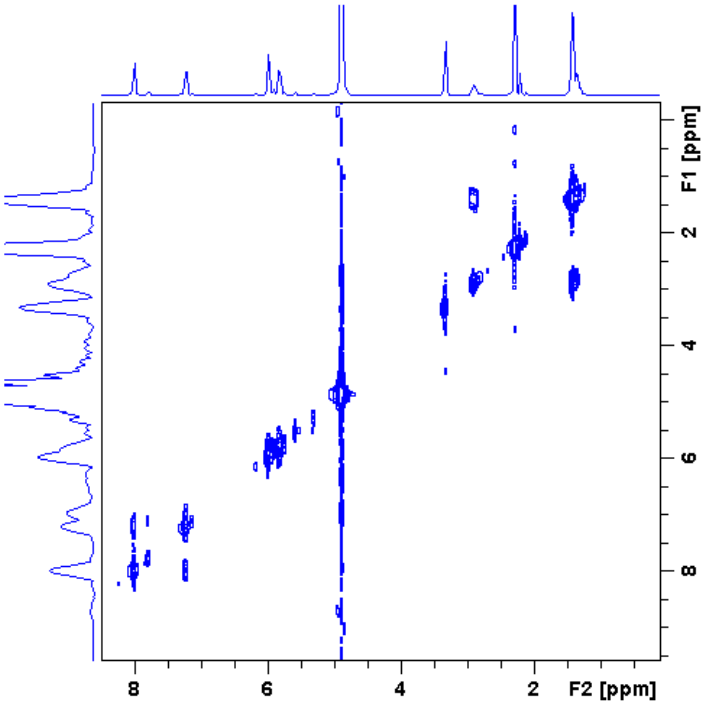

Fig. S4. ^{1}H-^{1}H COSY NMR spectrum of **MA$_1$** in CD_3OD at room temperature.

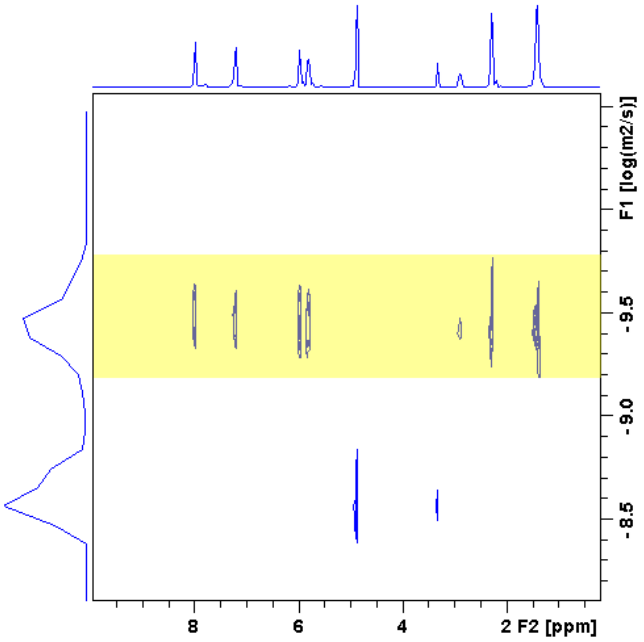

Fig. S5. DOSY NMR spectrum of **MA$_1$** in CD_3OD at room temperature.

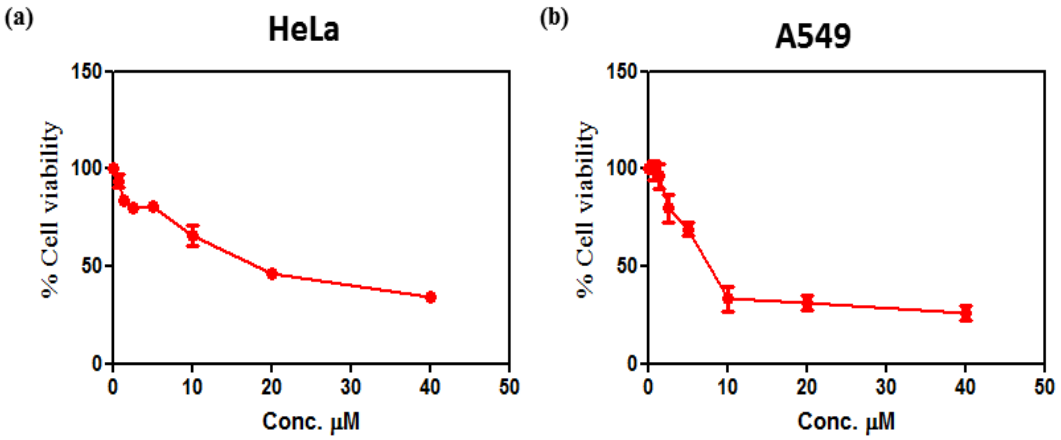

Fig. S6. Cell viability plots for the cytotoxicity of **MA_1.**

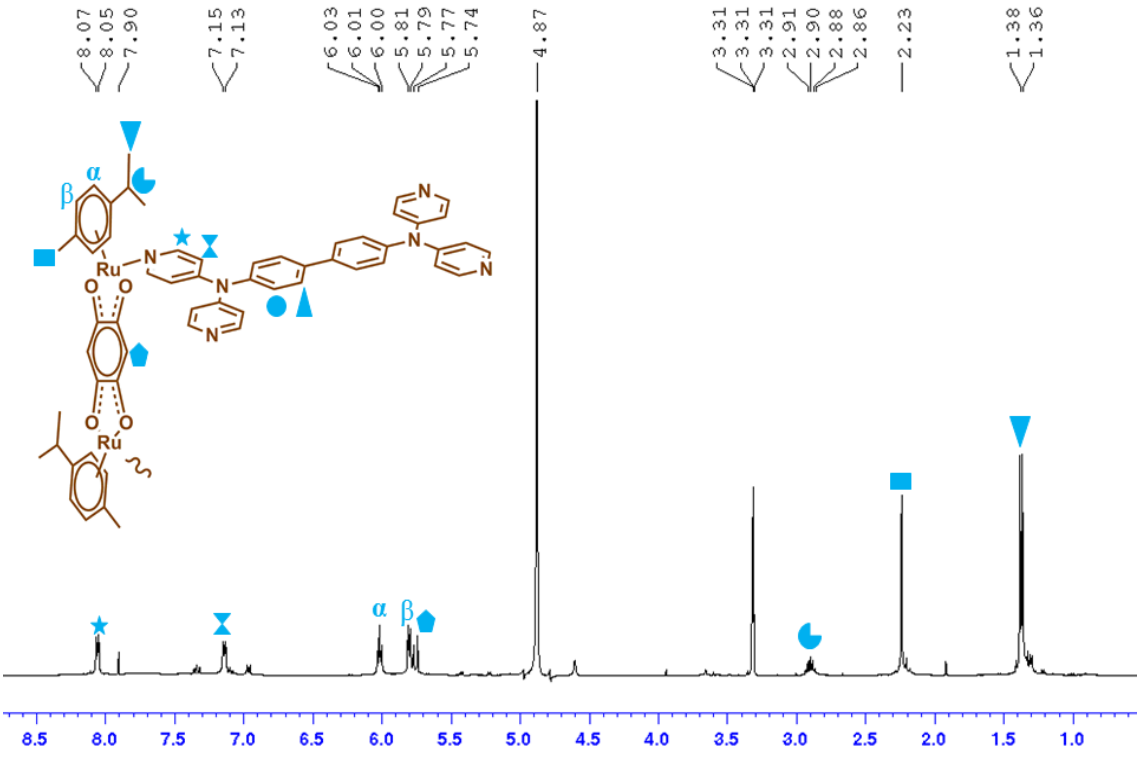

Fig. S7. ^{1}H NMR spectrum of **MA_2** in CD_3OD at room temperature.

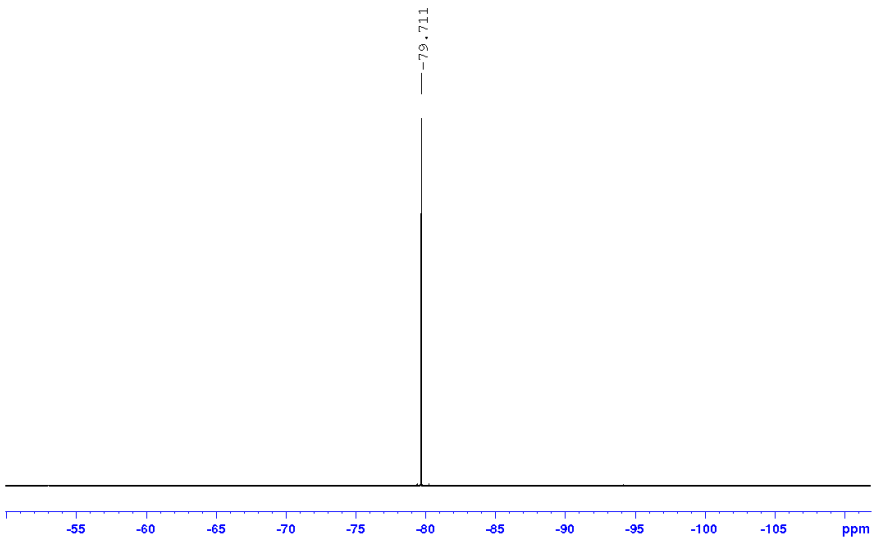

Fig. S8. ^{19}F NMR spectrum of **MA$_2$** in CD_3OD at room temperature.

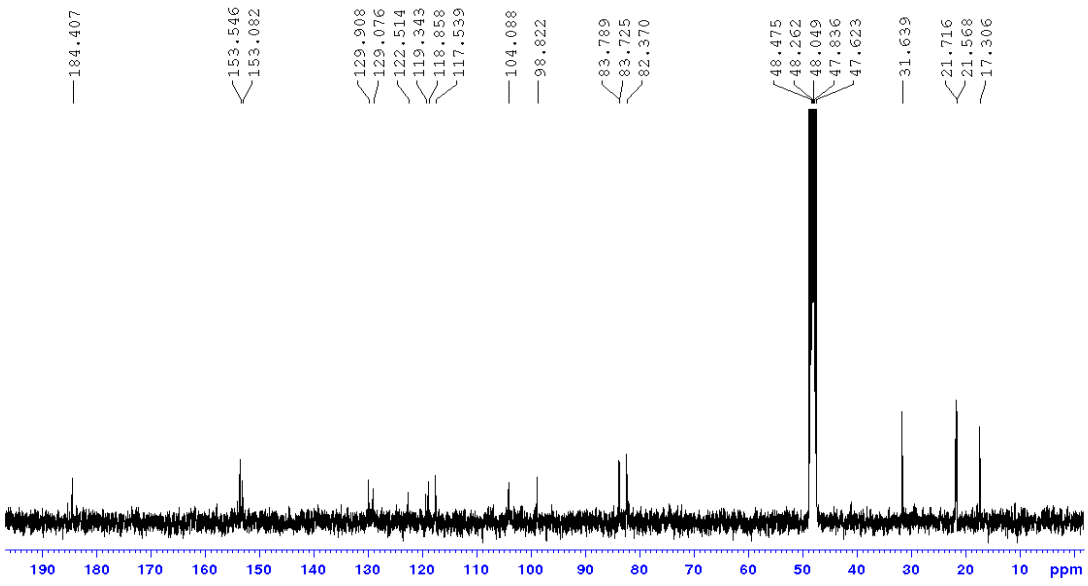

Fig. S9. ^{13}C NMR spectrum of **MA$_2$** in CD_3OD at room temperature.

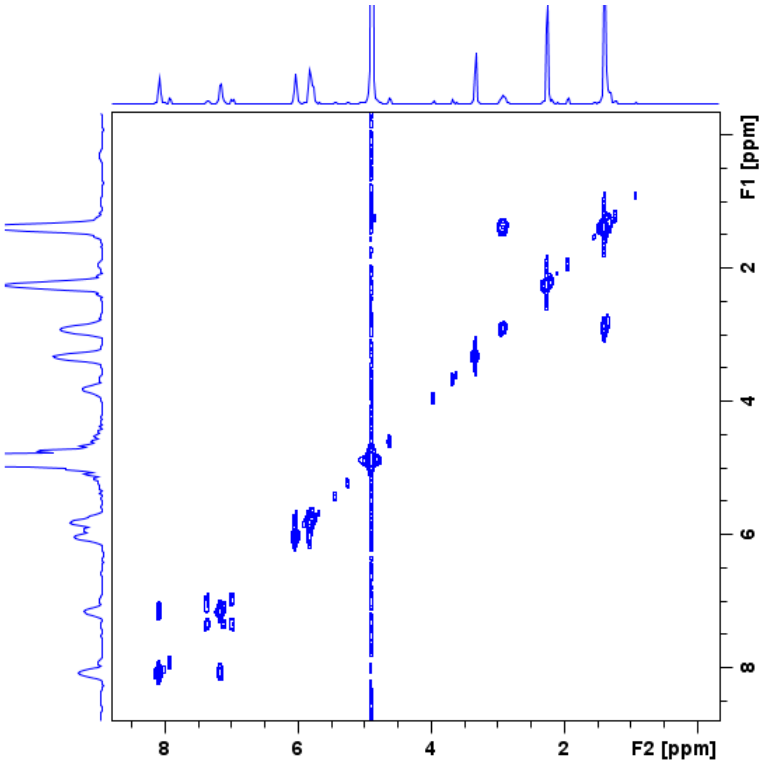

Fig. S10. ^{1}H-^{1}H COSY NMR spectrum of **MA$_2$** in CD_3OD at room temperature.

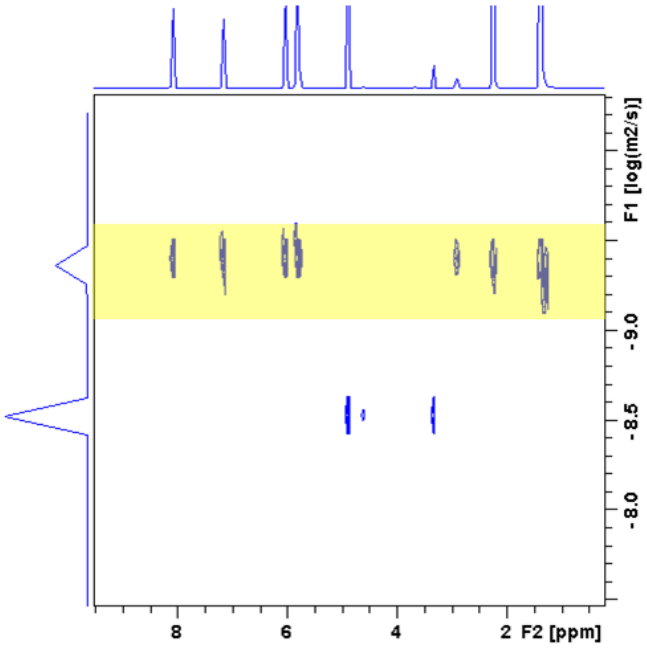

Fig. S11. DOSY NMR spectrum of **MA$_2$** in CD_3OD at room temperature.

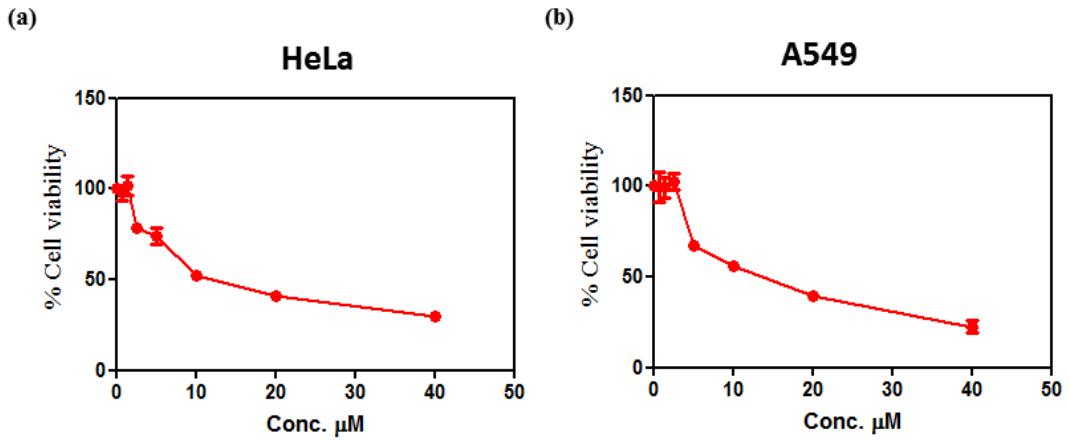

Fig. 12. Cell viability plots for the cytotoxicity of **MA_2.**

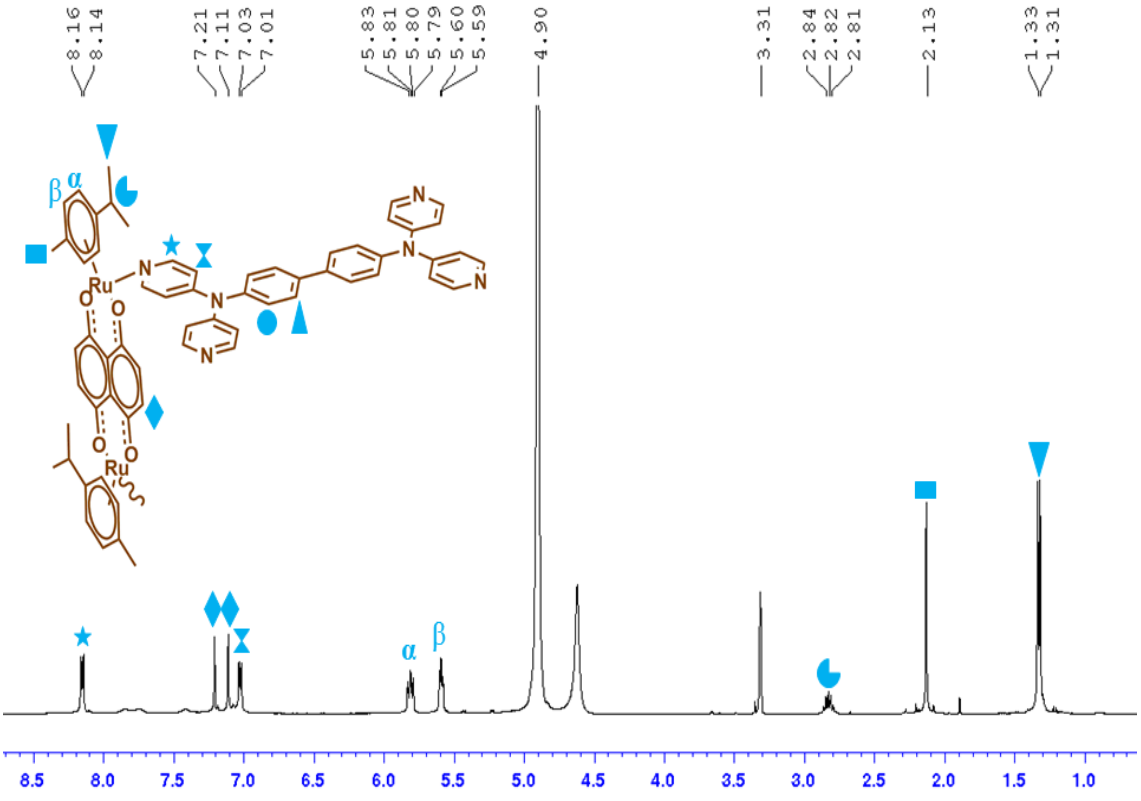

Fig. S13. ^{1}H NMR spectrum of **MA_3** in CD_3OD at room temperature.

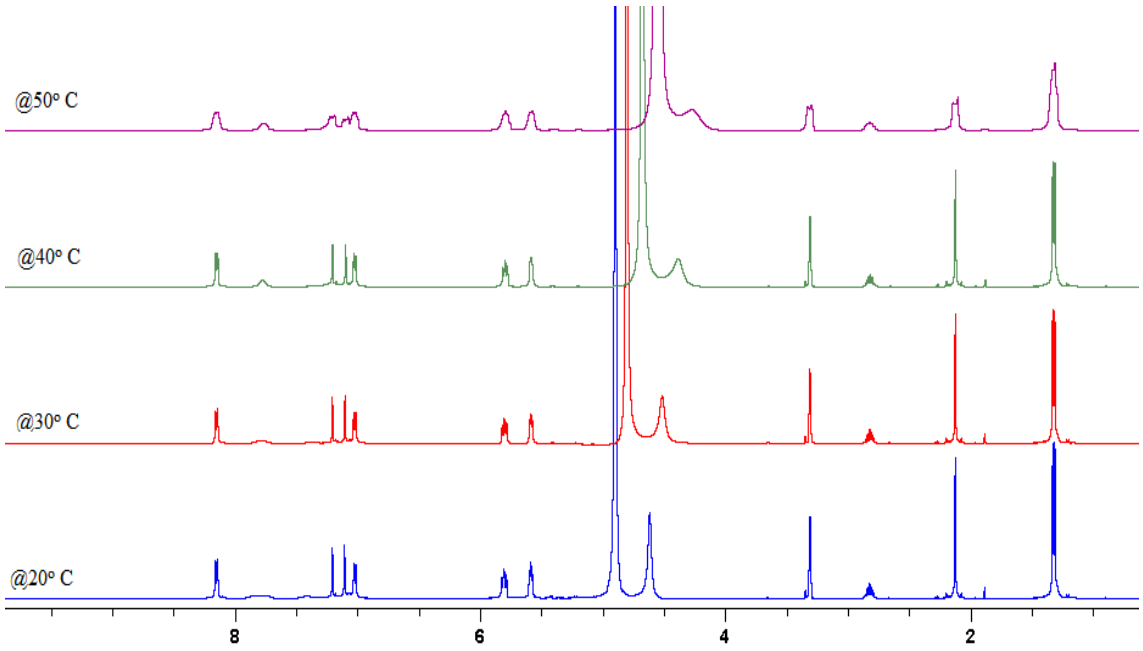

Fig. S14.Temperature-dependent ^{1}H NMR of **MA$_3$** in CD_3OD from 20° C to 50° C.

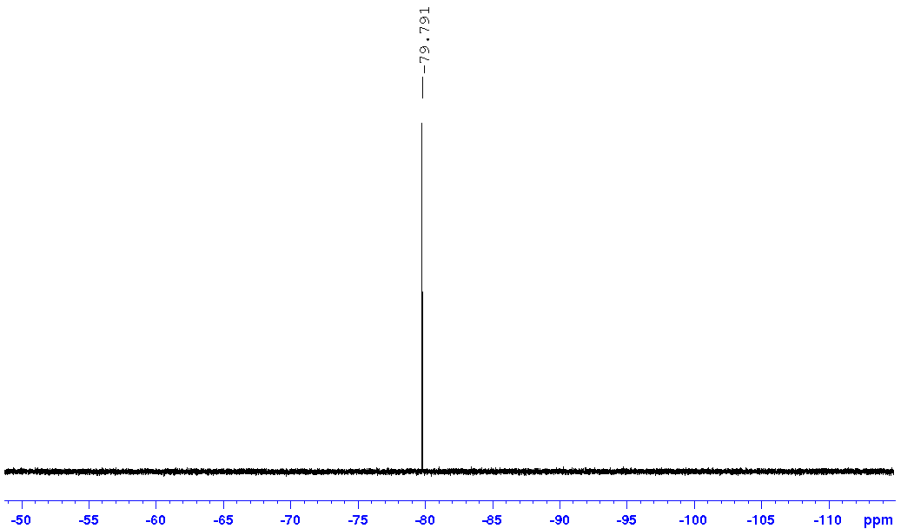

Fig. S15. ^{19}F NMR spectrum of **MA$_3$** in CD_3OD at room temperature.

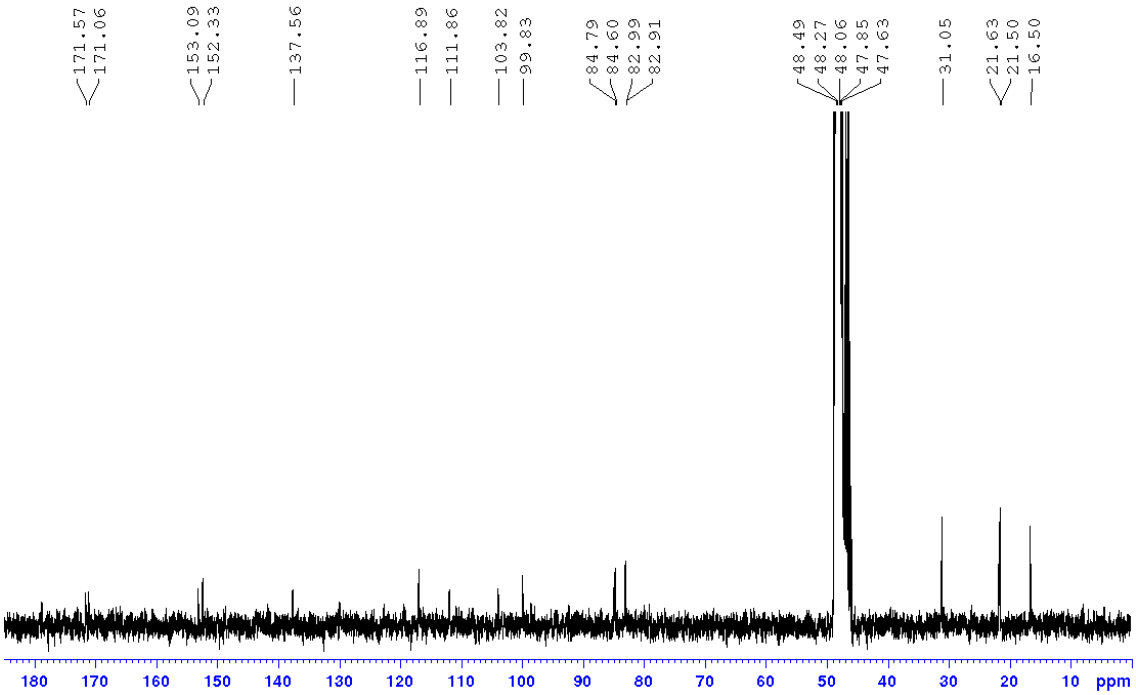

Fig. S16. ^{13}C NMR spectrum of **MA$_3$** in CD_3OD at room temperature.

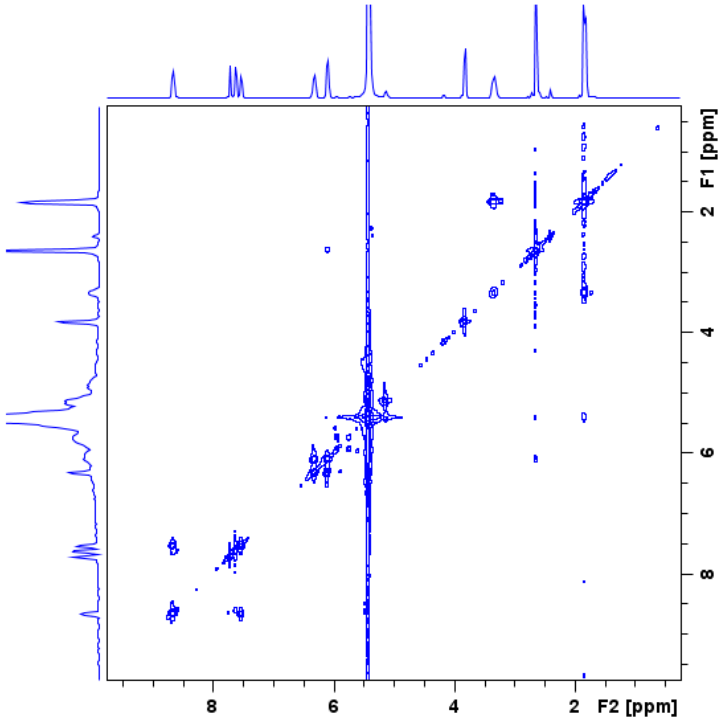

Fig. S17. ^{1}H-^{1}H COSY NMR spectrum of **MA$_3$** in CD_3OD at room temperature.

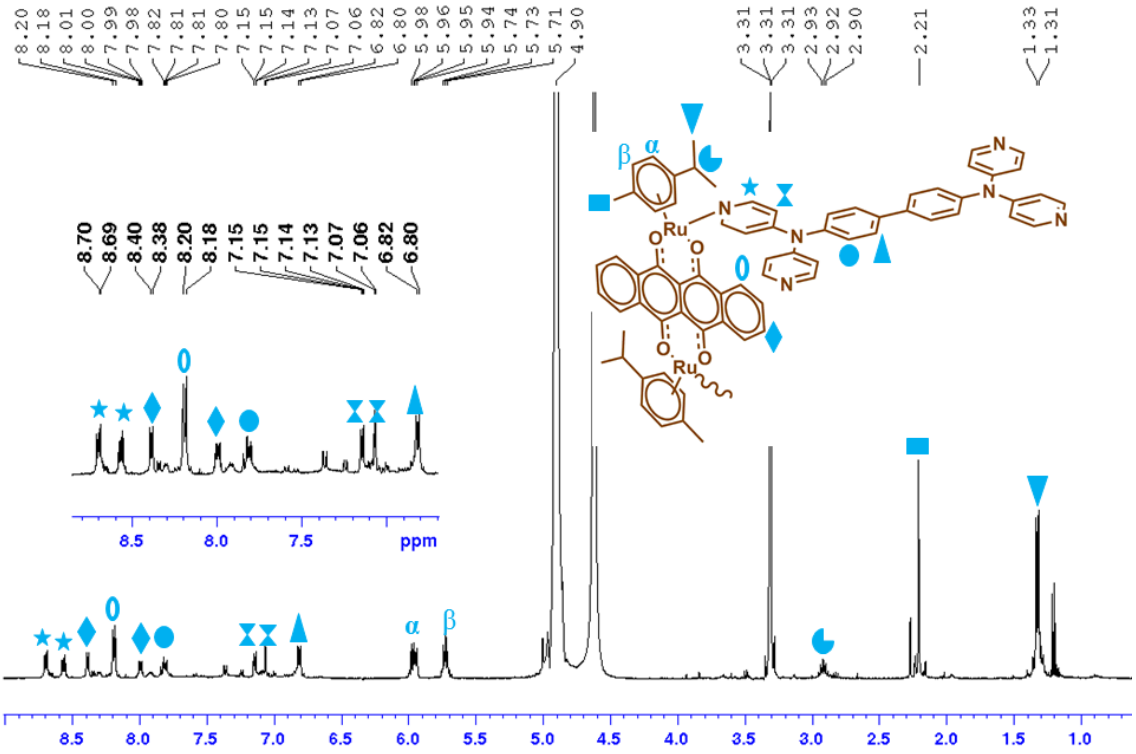

Fig. S18. ^{1}H NMR spectrum of **MA$_4$** in CD_3OD at room temperature.

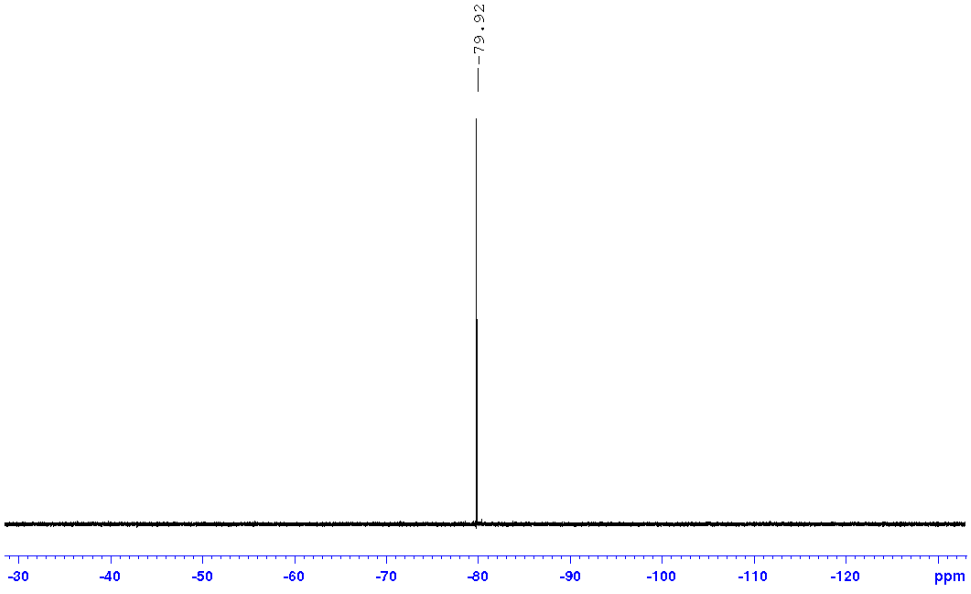

Fig. S19. ^{19}F NMR spectrum of **MA$_4$** in CD_3OD at room temperature.

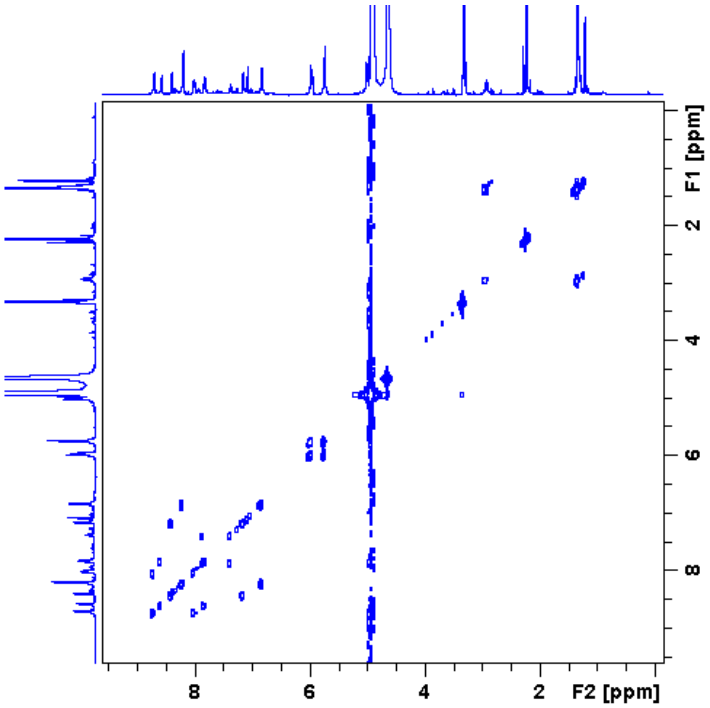

Fig. S20. ^{1}H-^{1}H COSY NMR spectrum of **MA$_4$** in CD_3OD at room temperature.

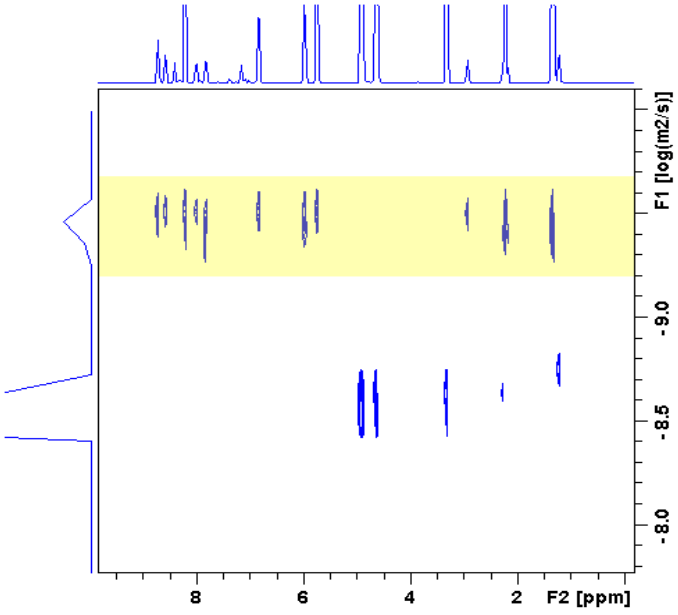

Fig. S21. DOSY NMR spectrum of **MA$_4$** in CD_3OD at room temperature.

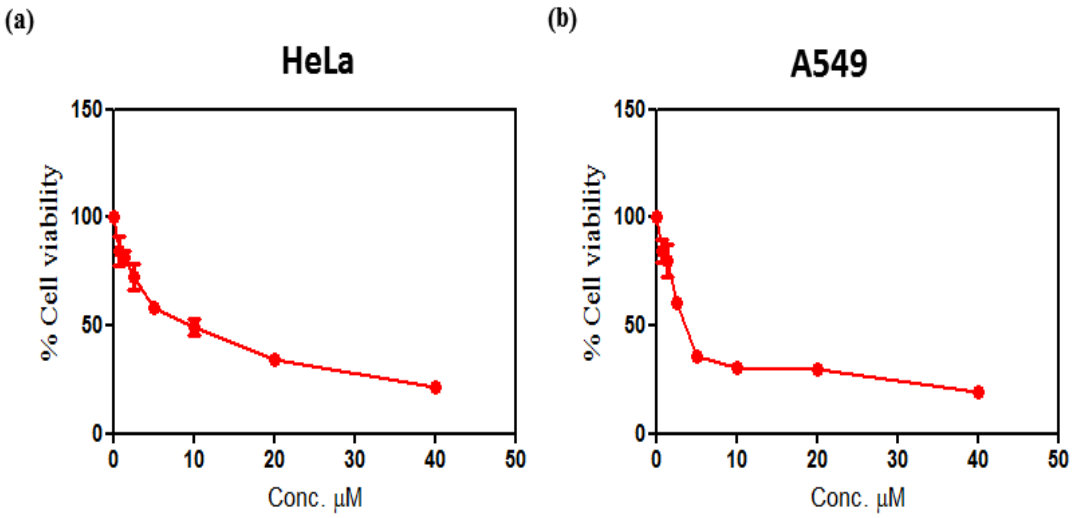

Fig. S22. Cell viability plots for the cytotoxicity of **MA4**.

The Stokes-Einstein equation was used calculate the hydrodynamic radius using the diffusion coefficient (D) obtained from the DOSY NMR experiment;

$$D = \frac{k_B T}{6\pi\eta r_H}$$

where, D = diffusion coefficient; k_B = Boltzmann constant (1.3806 x 10^{-23} $m^2Kgs^{-2}K^{-1}$); T = Absolute temperature (298 K); η = viscosity coefficient of CD_3OD (6.02 x 10^{-4} $Kgm^{-1}s^{-1}$); r_H = hydrodynamic radius. The respective values of r_H for supramolecular architectures MA_1, MA_2 and MA_4 as calculated from the above equation is summarized in table S1.

Table S1. Diffusion coefficients and hydrodynamic radii of **MA1 - MA4**.

Molecular Architecture	Diffusion coefficient (D)	Hydrodynamic radius (r_H)
MA1	-9.480 log (m^2s^{-1})	1.094 x 10^{-9} m (10.94 Å)
MA2	-9.375 log (m^2s^{-1})	8.661 x 10^{-10} m (8.66 Å)
MA3	-9.451 (logm^2s^{-1})	1.029 x 10^{-9} m (10.29 Å)
MA4	-9.465 log (m^2s^{-1})	1.063 x 10^{-9} m (10.63 Å)

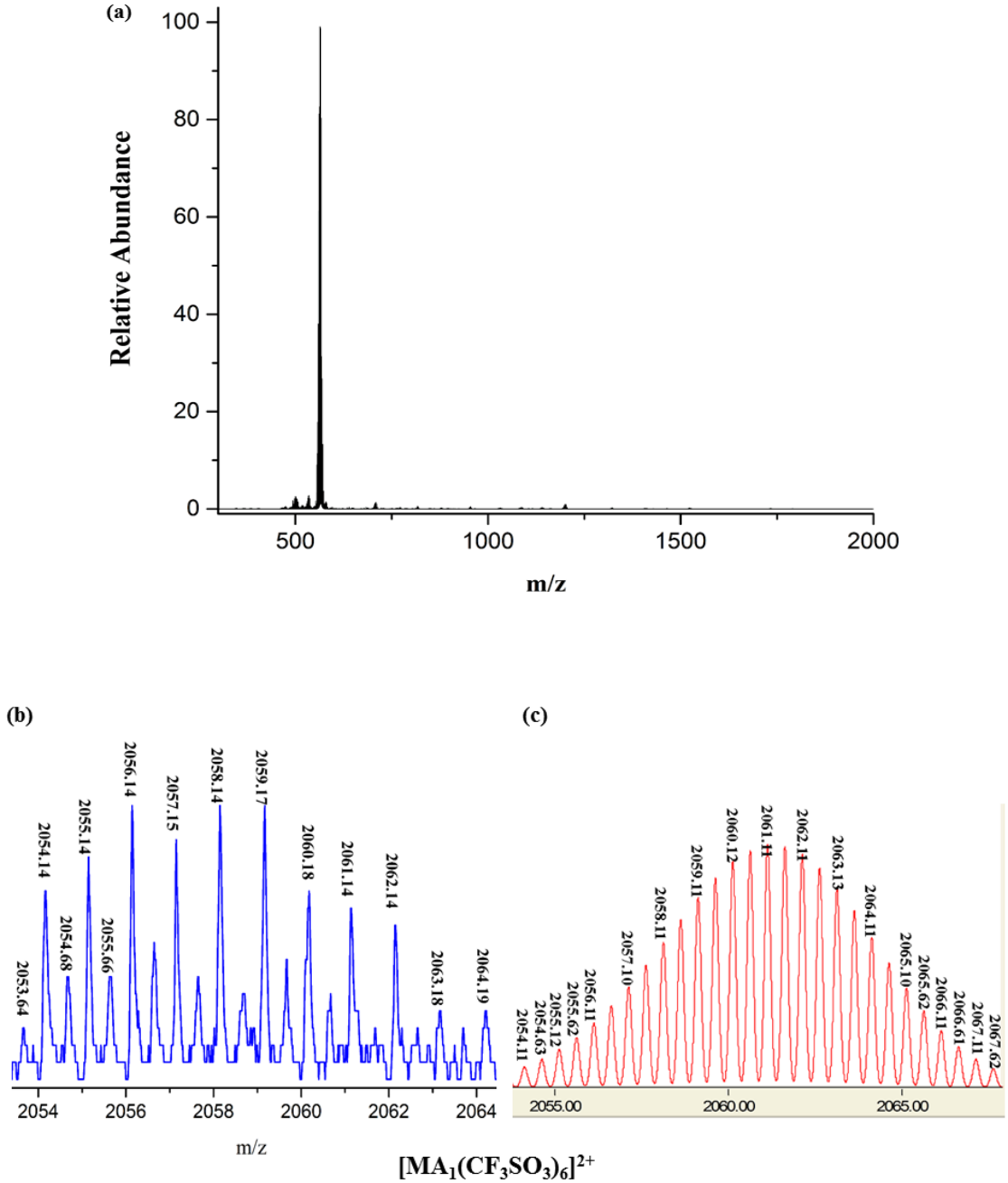
(a)
Relative Abundance
100
80
60
40
20
0
500
1000
1500
2000
m/z
(b)
2053.64
2054.14
2054.68
2055.14
2055.66
2056.14
2057.15
2058.14
2059.17
2060.18
2061.14
2062.14
2063.18
2064.19
2054
2056
2058
2060
2062
2064
m/z
(c)
2054.11
2054.63
2055.12
2055.62
2056.11
2057.10
2058.11
2059.11
2060.12
2061.11
2062.11
2063.13
2064.11
2065.10
2065.62
2066.11
2066.61
2067.11
2067.62
2055.00
2060.00
2065.00
[MA1(CF3SO3)6]2+

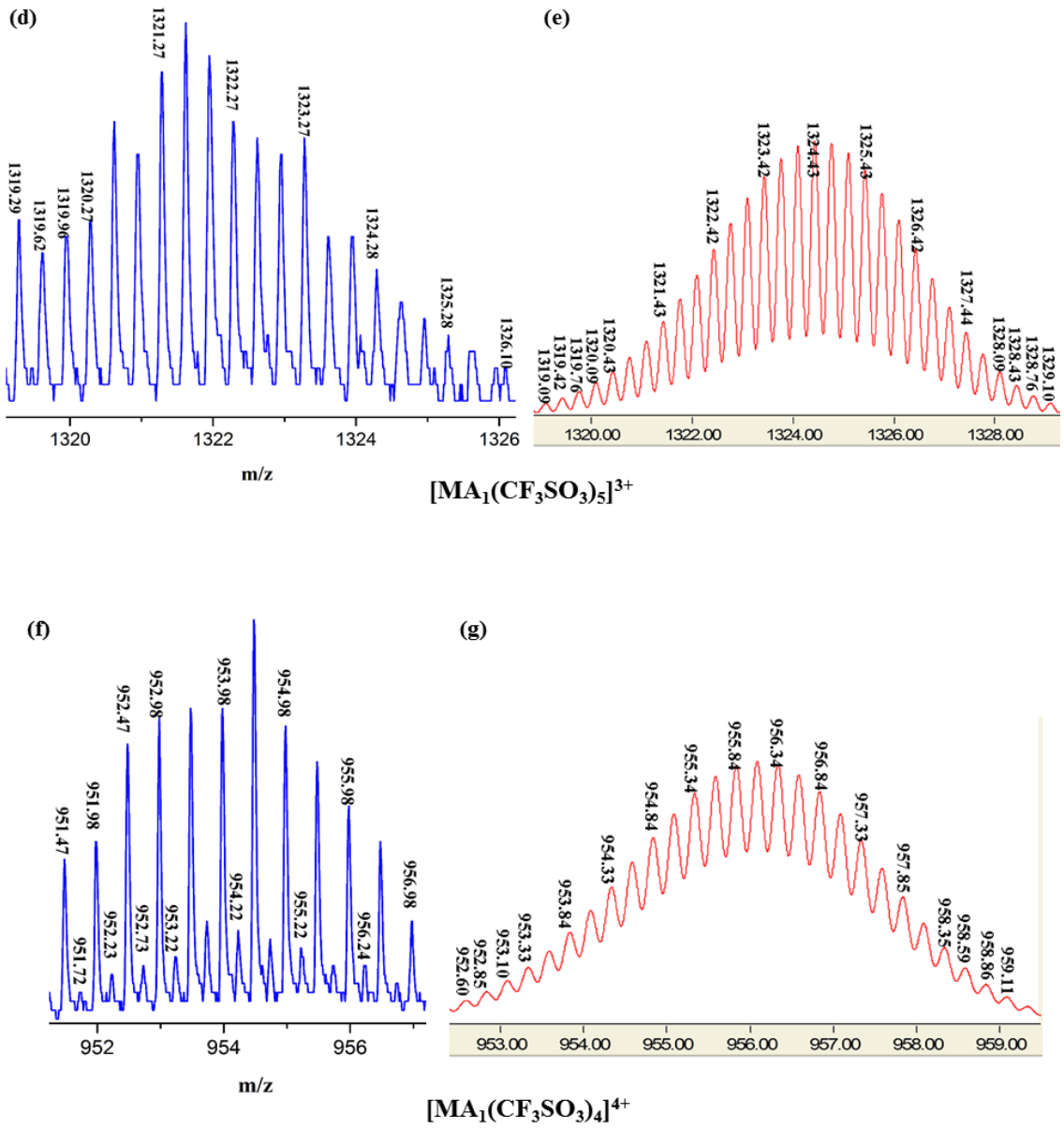

Fig. S23. (a) Full ESI-MS spectrum of **MA1** in methanol; (b), (d), (f) experimental and (c), (e), (g) theoretical isotopic distribution of the charged fragments.

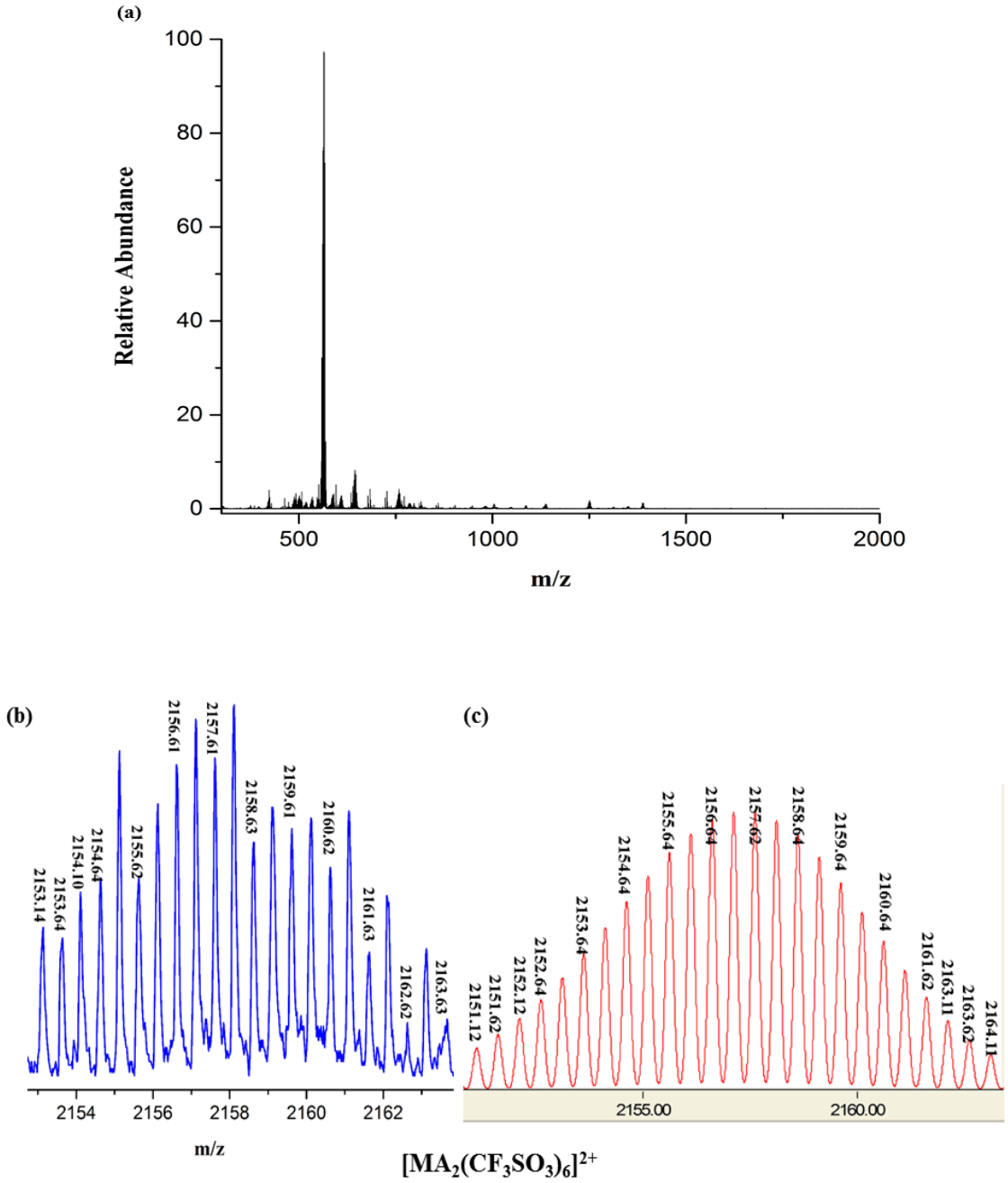
(a)
Relative Abundance
100
80
60
40
20
0
500
1000
1500
2000
m/z
(b)
2153.14
2153.64
2154.10
2154.64
2155.62
2156.61
2157.61
2158.63
2159.61
2160.62
2161.63
2162.62
2163.63
2154
2156
2158
2160
2162
m/z
(c)
2151.12
2151.62
2152.12
2152.64
2153.64
2154.64
2155.64
2156.64
2157.62
2158.64
2159.64
2160.64
2161.62
2163.11
2163.62
2164.11
2155.00
2160.00
[MA2(CF3SO3)6]2+

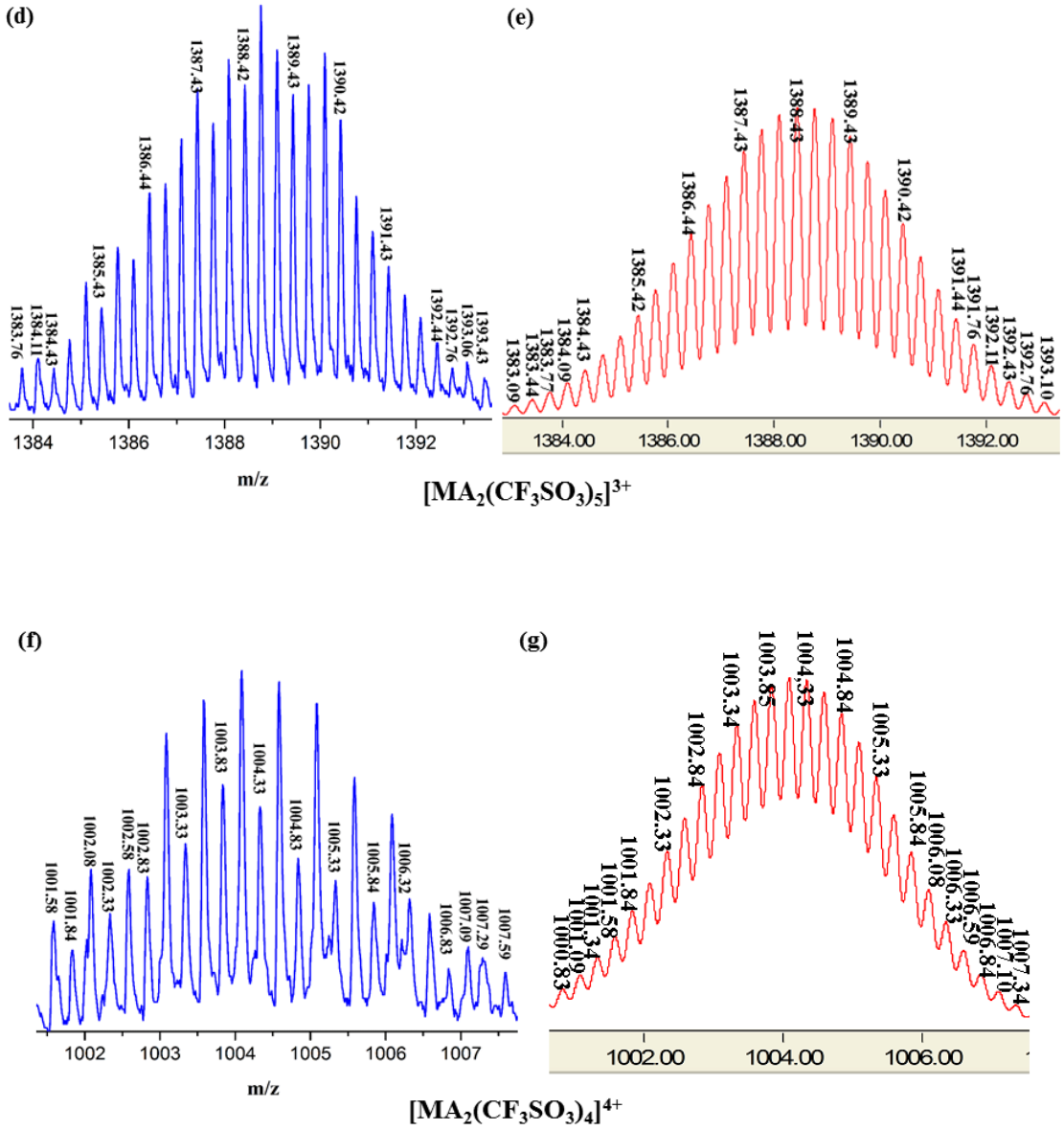

Fig. S24. (a) Full ESI-MS spectrum of **MA2** in methanol; (b), (d), (f) experimental and (c), (e), (g) theoretical isotopic distributions of the charged fragments.

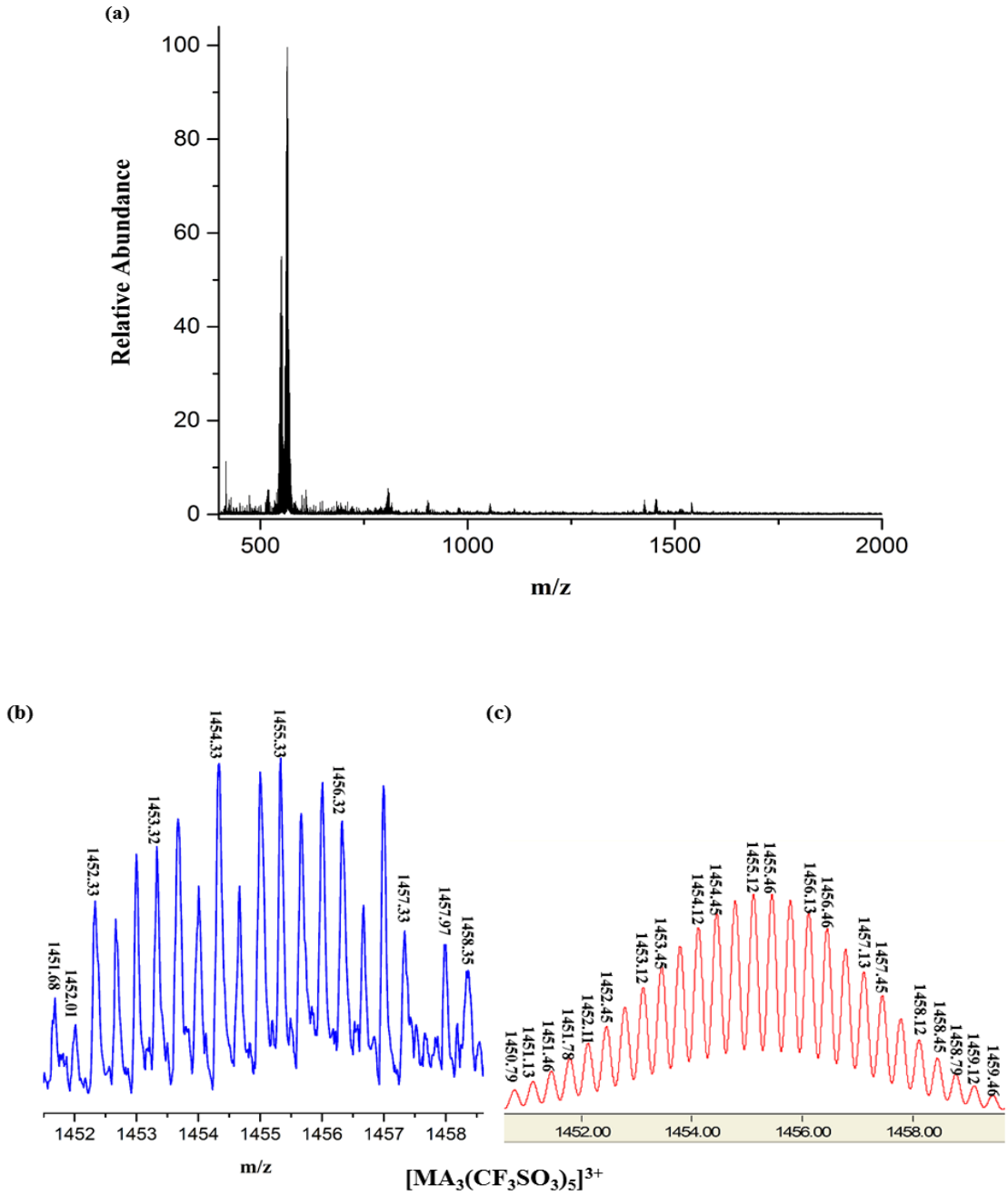
(a)
Relative Abundance
100
80
60
40
20
0
500
1000
1500
2000
m/z
(b)
1451.68
1452.01
1452.33
1453.32
1454.33
1455.33
1456.32
1457.33
1457.97
1458.35
1452
1453
1454
1455
1456
1457
1458
m/z
(c)
1450.79
1451.13
1451.46
1451.78
1452.11
1452.45
1453.12
1453.45
1454.12
1454.45
1455.12
1455.46
1456.13
1456.46
1457.13
1457.45
1458.12
1458.45
1458.79
1459.12
1459.46
1452.00
1454.00
1456.00
1458.00
[MA3(CF3SO3)5]3+

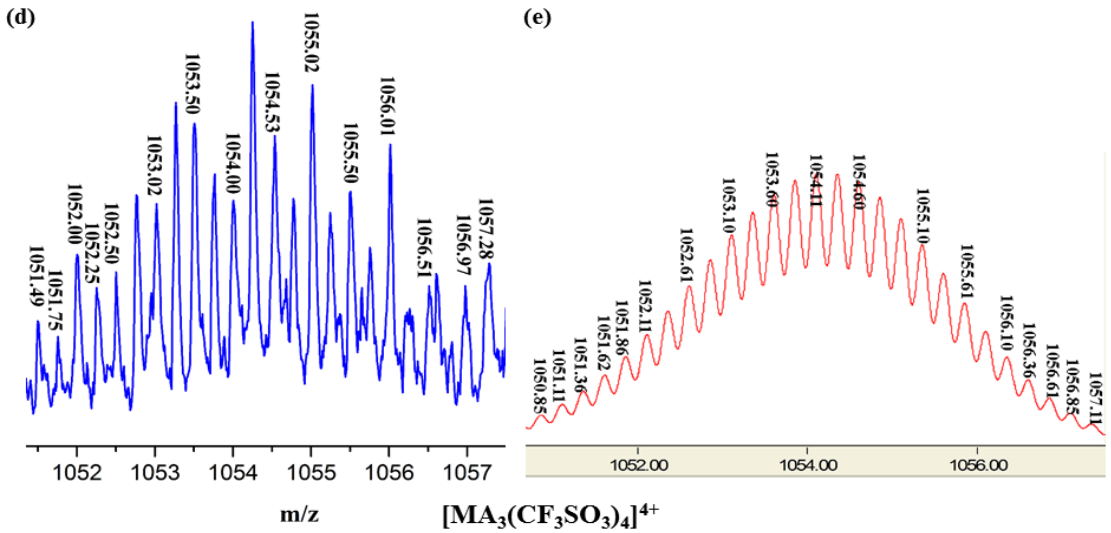

Fig. S25. (a) Full ESI-MS spectrum of **MA$_3$** in methanol; (b), (d) experimental and (c), (e) theoretical isotopic distribution of the charged fragments.

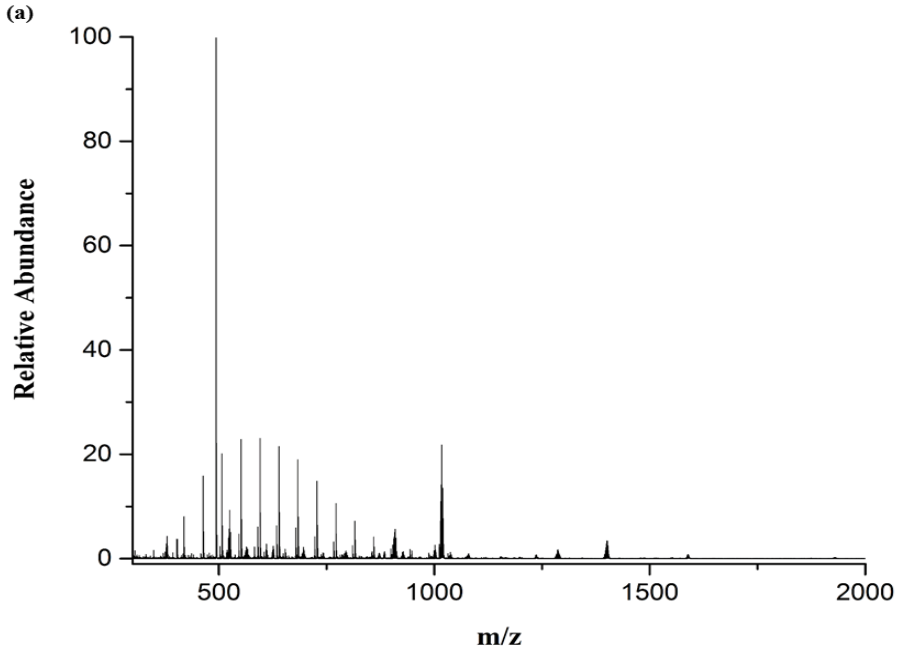

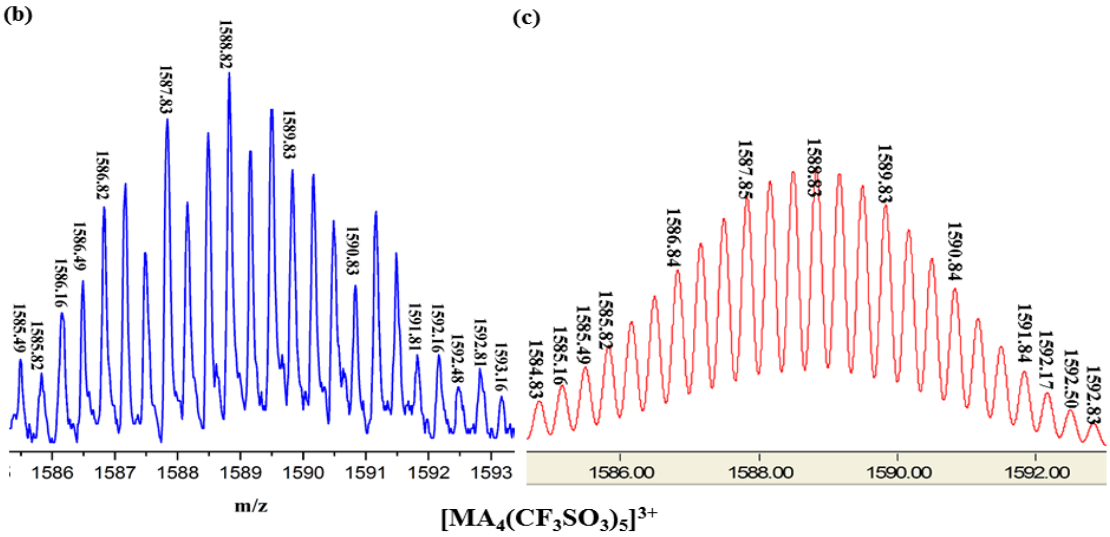

Fig. S26. (a) Full ESI-MS spectrum of **MA4** in methanol; (b) experimental and (c) theoretical isotopic distribution of the charged fragment.

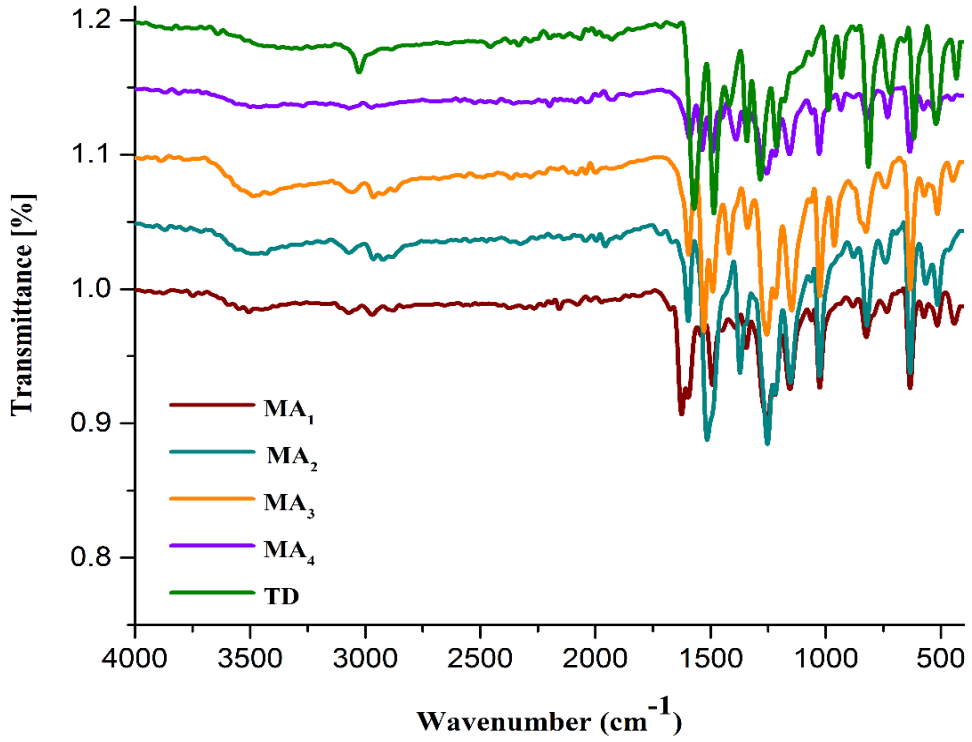

Fig. S27. FTIR spectra of **TD** and **MA1 - MA4.**

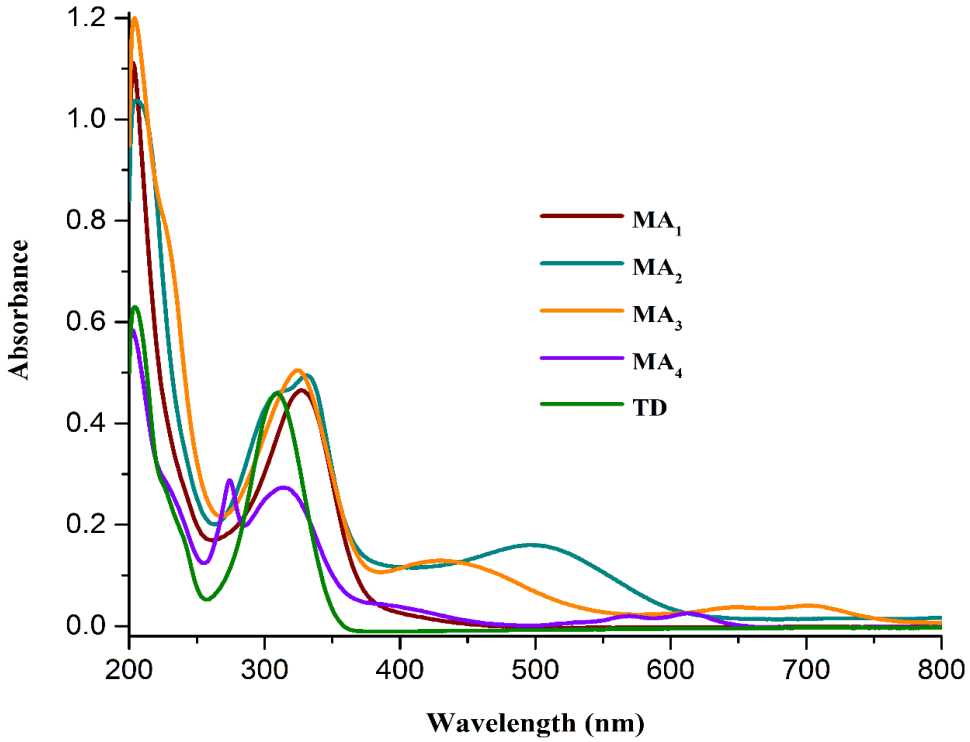

Fig. S28. UV-Vis absorption spectra of **TD** and **MA1 - MA4** recorded in methanol (3.5×10^{-5} M) at 298 K.

Table S2. Selected bond lengths [Å] and angles [°] for MA_1.

Bond lengths [Å]		**Bond angles [°]**	
Ru01-N00I	2.103(5)	N00I-Ru01-O00B	81.60(2)
Ru01-O00B	2.122(5)	N00I-Ru01-O00C	87.20(2)
Ru01-O00C	2.111(5)	O00C-Ru01-O00B	78.57(18)
Ru02-N00L	2.096(5)	N00L-Ru02-O008	82.61(19)
Ru02-O008	2.131(4)	N00L-Ru02-O00E	85.70(2)
Ru02-O00E	2.100(5)	O00E-Ru02-O008	78.98(18)
Ru03-N00J	2.098(5)	N00J-Ru03-O009	81.65(19)
Ru03-O009	2.111(4)	N00J-Ru03-O00D	87.10(2)
Ru03-O00D	2.136(5)	O009-Ru03-O00D	78.15(18)
Ru04-N00N	2.105(6)	N00N-Ru04-O00A	79.80(2)
Ru04-O00A	2.106(4)	N00N-Ru04- O00F	85.80(2)
Ru04-O00F	2.101(5)	O00F-Ru04-O00A	78.90(18)

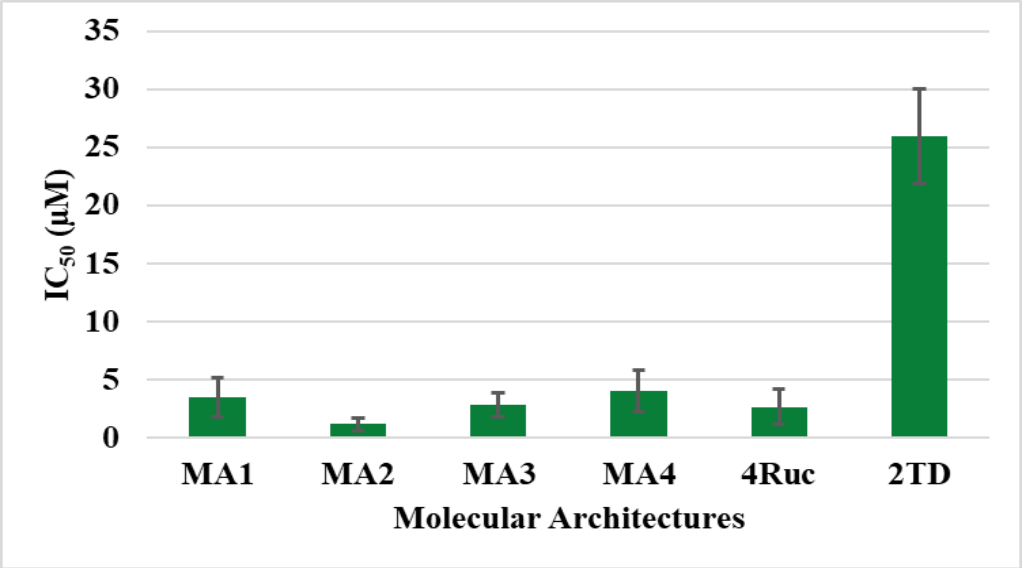

Chart S1. IC_{50} values (µM) of **MA_1 – MA_4, Ru_c** and **TD** on normal lung epithelial cells HPL1D

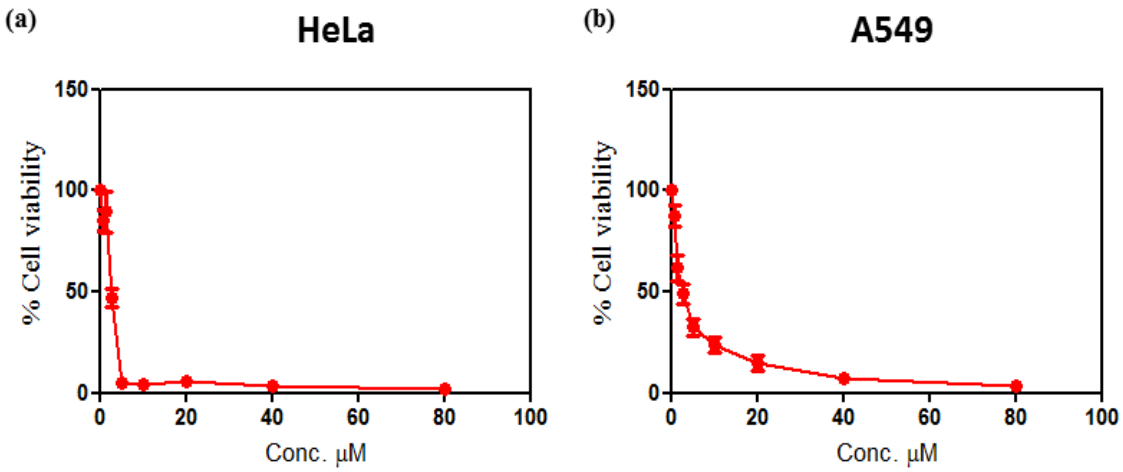

Fig. S29. Cell viability plots for the cytotoxicity of **Ru_c**.

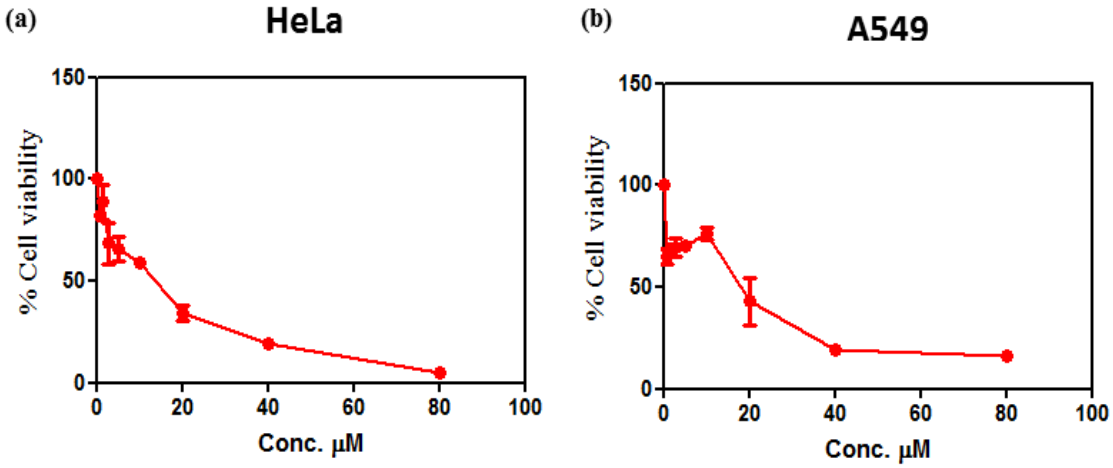

Fig. S30. Cell viability plots for the cytotoxicity of **TD**.